SCIENCE CHINA
Technological Sciences

August 2012 Vol.55 No.8: 2362–2376
doi: 10.1007/s11431-012-4888-4

Consolidation and dynamics of 3D unsaturated porous seabed under rigid caisson breakwater loaded by hydrostatic pressure and wave

YE JianHong[1*], JENG DongSheng[1] & CHAN A H C[2]

[1] *Division of Civil Engineering, University of Dundee, Dundee DD1 4HN, UK;*
[2] *Department of Civil Engineering, University of Birmingham, Birmingham, B15 2TT, UK*

Received July 27, 2011; accepted April 9, 2012; published online June 15, 2012

In this study, based on the dynamic Biot's theory "*u-p*" approximation, a 3D finite element method (FEM) numerical soil model is developed, in which the Generalized Newmark-β method is adopted to determine the time integration. The developed 3D FEM soil model is a part of the coupled model PORO-WSSI 3D for 3D wave-seabed-marine structures interaction problem, and is validated by the analytical solution proposed by Wang (2000) for a laterally infinite seabed loaded by a uniform force. By adopting the developed 3D soil model, the consolidation of seabed under a caisson breakwater and hydrostatic pressure is investigated. The numerical results show that the caisson breakwater built on seabed has very significant effect on the stresses/displacements fields in the seabed foundation after the transient deformation and primary consolidation are completed. The parametric study indicates that the Young's modulus E of seabed is the most important parameter to affect the settlement of breakwater, and the displacement fields in seabed foundation. Taking the consolidation status as the initial condition, the interaction between ocean wave, caisson breakwater and seabed foundation is briefly investigated. The 3D ocean wave is determined by solving the Navier-Stokes equations with finite volume method (FVM). The numerical results indicate that there is intensive interaction between ocean wave, caisson breakwater and seabed foundation; and the breakwater indeed can effectively block the wave energy propagating to the coastline.

consolidation, wave-seabed-breakwater interaction, unsaturated seabed, breakwater, Biot's theory, Navier-Stokes equation

Citation: Ye J H, Jeng D S, Chan A H C. Consolidation and dynamics of 3D unsaturated porous seabed under rigid caisson breakwater loaded by hydrostatic pressure and wave. Sci China Tech Sci, 2012, 55: 2362–2376, doi: 10.1007/s11431-012-4888-4

1 Introduction

Nowadays, more than two-thirds of the world's population is concentrated in the coastal zones, where the coastline generally is either the center of economic development, or the important port for transportation. In coastal zones, the breakwaters, such as caisson breakwater, are widely used to protect the coastline from damage and erosion; and also could protect the people living in the zones near to the coastline from death and properties loss induced by the probable tsunami attack. However, the breakwaters built on porous seabed are vulnerable to the liquefaction and the shear failure of seabed foundation [1–3]. In engineering, an inappropriate design of the breakwater would result in the collapse of breakwater after construction, and further bring great economic loss. Therefore, it is meaningful to develop an effective analysis tool for coastal engineers to predict and evaluate the stability of seabed foundation under marine structures.

In recent three decades, more and more marine structures, such as breakwater, oil platform and turbine, have been

*Corresponding author (email: yejianhongcas@gmail.com or JZYE@dundee.ac.uk)

constructed in offshore areas. The response of seabed foundation under the gravity of marine structures and the ocean wave/earthquake becomes the main issue most concerned by coastal engineers involved in design of marine structures. Since 1970s, a great number of works have been conducted in the field of ocean soil mechanics. A series of valuable results have been obtained. Among these, Yamamoto et al. (1978) [4] derived an analytical solution for linear wave-induced dynamic response of an isotropic, poro-elastic and infinite seabed by treating the pore water and seabed as compressible and deformable medium. Later, Hsu and Jeng (1994) [5] further extended the framework to the unsaturated, isotropic seabed with finite thickness under three-dimensional short crested waves loading. Recently, Ulker (2009) [6] proposed a similar analytical solution for the dynamic response of a finite seabed under linear wave, in which the acceleration of both soil particles and pore water is considered. Unfortunately, the marine structures built on seabed cannot be considered; and the gravity of seabed soil is not included in these analytical solutions. In engineering, the numerical modeling is another powerful tool, which could consider the effect of marine structures, and include the gravity term in governing equations for porous medium. Jeng et al. (2001) [7] developed a 2D finite element method (FEM) model to investigate the dynamic wave-induced pore pressure in seabed under a linear wave around a composite breakwater built on a finite, isotropic and homogeneous seabed. However, the effect of gravity of the composite breakwater on the seabed response, and the effect of composite breakwater on the wave train were not considered. Later, Mizutani et al. (1998) [8] and Mostafa et al. (1999) [9] developed a 2D BEM-FEM integrated numerical model to investigate the interaction between the wave-seabed-structures based on the Laplace's equation for fluid and the Biot's consolidation equation for porous seabed. In the BEM-FEM integrated model, the gravity of breakwater, and the effect of breakwater on the wave train can be considered. Recently, Ye et al. (2012) [10] also developed a 2D integrated numerical model (PORO-WSSI II) to investigate the liquefaction process of seabed foundation beneath a composite breakwater under various waves, such as regular wave, solitary wave and breaking wave. In PORO-WSSI II, the Navier-Stokes equations govern the seawater and are solved by finite difference method; and the dynamic Biot's equation "*u-p*" approximation governs the porous seabed and is solved by finite element method.

It is well known that the seabed generally has experienced the consolidation process under the hydrostatic pressure and the self-gravity in the geological history in the offshore environment. In engineering, after the construction of a breakwater on seabed, the gravity of breakwater is initially transferred to the pore water in seabed foundation, resulting in the generation of excess pore pressure and pressure gradient. As time passing by, the pore water permeates driven by the pressure gradient through the void between soil particles, promoting the pore pressure to dissipate gradually. In this process, the gravity of breakwater gradually is transferred from the pore water to the soil particles; and the breakwater subsides correspondingly. Finally, the seabed foundation reaches a new consolidation status, which should be taken as the initial conditions for the evaluation of the dynamic response of seabed foundation and breakwater under ocean wave or earthquake loading. Most of the previous investigations mainly paid their attention to the seabed dynamic response; however, it is assumed that all the initial values, including the displacements, velocity, stresses and pore pressure are all zero [7, 8, 9, 11, 12]. Obviously, the assumption made by previous investigations is not consistent with the real situations. Actually, the stresses and pore pressure in seabed foundation absolutely are not zero at the beginning stage of construction. This assumption would make the evaluation of liquefaction and dynamic shear failure of seabed foundation under wave/earthquake loading lowly reliable. The determination of the initial consolidation status of seabed foundation under hydrostatic pressure and breakwater is significantly necessary, and is one of the key steps in evaluation of the stability of seabed foundation and marine structures [10].

The first researcher investigating the consolidation problem was Terzaghi [13] who proposed the analytical solution of 1D soil volume consolidating under a constant pressure. Later Biot [14, 15] presented a 3D general theory for the soil consolidation, which has been widely adopted to understand the coupled phenomenon between the flow and the deformed porous media. Generally, the exact solution of consolidation problems of soil is difficult to obtain due to the complex boundary conditions. In engineering, most problems are solved by numerical techniques. At present, a lot of literatures are available about the Biot's consolidation theory. However, most of them pay their attention to the methods of solving the 2D Biot's consolidation equation, and the corresponding convergence and numerical stability [16–21]. Little attention has been given to the application of these numerical methods proposed to determination of the consolidation status of large-scale seabed foundation under hydrostatic pressure and large-scale breakwater. Furthermore, the 2D numerical model is not applicable to the determination of the consolidation status of seabed foundation beneath the head of a breakwater. In this case, the 3D model is urgently needed. Additionally, the acceleration of soil particles and pore water cannot be considered in previous models.

In this study, the Biot's dynamic equation (known as "*u-p*" approximation) proposed by Zienkiewicz et al. (1980) [22] is taken as the governing equation for the porous seabed. The acceleration of soil particles and pore water is considered. A 3D FEM numerical soil model (part of a 3D coupled model PORO-WSSI 3D) is developed, in which the Generalized Newmark-β method is used to determine the time integration. By adopting the developed 3D soil model,

the consolidation of 3D seabed foundation under hydrostatic pressure and a caisson breakwater is intensively investigated. Generally, the consolidation of seabed under marine structures includes transient deformation, primary consolidation and secondary consolidation. The transient deformation and primary consolidation of a sandy seabed are mainly related to the elasticity of seabed. The secondary consolidation of seabed is dominantly related to the plasticity and creep. In this study, only the transient deformation of primary consolidation of seabed foundation under a caisson breakwater is studied. After the consolidation status of seabed foundation is determined, taking the consolidation status as the initial condition, the ocean wave-caisson breakwater-seabed foundation interaction is investigated. The 3D ocean wave is determined by solving the Navier-Stokes equations with finite volume method (FVM). It is noted that the compressive stress is taken as negative value; and the displacement with the same direction with axis is defined as positive in this study.

2 Boundary value problem

2.1 Governing equation

It is well known that the seabed is porous medium consisting of the soil particles, pore water and trapped air. The Biot's theory is widely adopted to describe the mechanical behaviours of porous medium. In this study, the dynamic Biot's equation known as "*u-p*" approximation proposed by Zienkiewicz et al. (1980) [22] is used as the governing equation for 3D porous seabed. The relative displacements of pore water to the soil particles are ignored, however, the acceleration of the pore water and soil particles is considered in the governing equation.

The equilibrium equations are:

$$\frac{\partial \sigma'_x}{\partial x}+\frac{\partial \tau_{xy}}{\partial y}+\frac{\partial \tau_{xz}}{\partial z}=-\frac{\partial p_s}{\partial x}+\rho\frac{\partial^2 u_s}{\partial t^2}, \tag{1}$$

$$\frac{\partial \tau_{xy}}{\partial x}+\frac{\partial \sigma'_y}{\partial y}+\frac{\partial \tau_{yz}}{\partial z}=-\frac{\partial p_s}{\partial y}+\rho\frac{\partial^2 v_s}{\partial t^2}, \tag{2}$$

$$\frac{\partial \tau_{xz}}{\partial x}+\frac{\partial \tau_{yz}}{\partial y}+\frac{\partial \sigma'_z}{\partial z}+\rho g=-\frac{\partial p_s}{\partial z}+\rho\frac{\partial^2 w_s}{\partial t^2}. \tag{3}$$

The mass continuity of pore water is:

$$k\nabla^2 p-\gamma_w n\beta\frac{\partial p_s}{\partial t}+k\rho_f\frac{\partial^2 \varepsilon}{\partial t^2}=\gamma_w\frac{\partial \varepsilon}{\partial t}. \tag{4}$$

In the above equations, u_s, v_s, w_s are the soil displacements in the x, y, z directions, respectively; n is soil porosity; σ'_x, σ'_y and σ'_z are the effective normal stresses in the horizontal and vertical directions, respectively; τ_{xy}, τ_{yz} and τ_{xz} are the shear stresses; p_s is the pore pressure in porous medium; $\rho=n\rho_f+(1-n)\rho_s$ is the average density of porous medium; ρ_f is the fluid density; ρ_s is solid density; k is the Darcy's permeability; g is the gravitational acceleration and γ_w is the unit water weight. ε is the volumetric strain. In eq. (4), the compressibility of pore fluid (β) and the volume strain (ε) are defined as

$$\varepsilon=\frac{\partial u_s}{\partial x}+\frac{\partial v_s}{\partial y}+\frac{\partial w_s}{\partial z}, \tag{5}$$

$$\beta=\frac{1}{K_f}+\frac{1-S_r}{p_{w0}}, \tag{6}$$

where S_r is the degree of saturation of seabed, p_{w0} is the absolute static pressure and K_f is the bulk modulus of pore water.

If the seabed has anisotropic permeability, k is expressed as

$$k=\begin{bmatrix} k_x & 0 & 0 \\ 0 & k_y & 0 \\ 0 & 0 & k_z \end{bmatrix}. \tag{7}$$

For isotropic porous seabed, the permeability coefficients should be the same at three directions: $k_x=k_y=k_z$.

2.2 Boundary conditions

In this study, the consolidation of a 3D porous unsaturated seabed ($L\times W\times H$: 250 m×130 m×15 m) under a rigid caisson breakwater ($W\times L\times H$: 10 m×90 m×16 m) is numerically investigated. The configuration of seabed and caisson breakwater in computational domain is shown in Figure 1. In order to solve the governing equations (1) to (4), the following boundary conditions are applied to the computational domain.

First, the bottom of seabed is rigid and impermeable:

$$u_s=v_s=w_s=0 \quad \text{and} \quad \frac{\partial p_s}{\partial z}=0 \quad \text{at} \quad z=0. \tag{8}$$

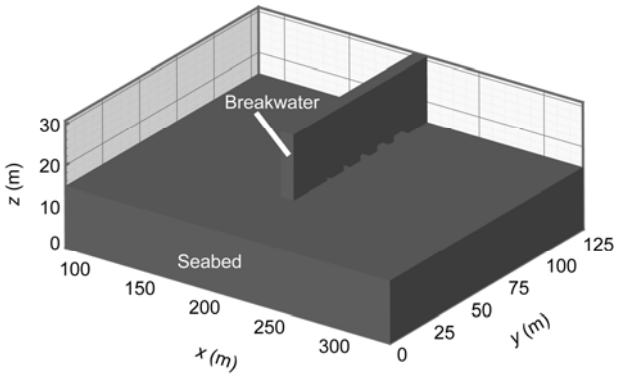

Figure 1 Computational domain in this study, in which a rigid caisson breakwater is built on seabed.

Second, due to the fact that the computational domain is symmetrical along x direction (symmetrical plane x=205 m), and the computational domain is truncated from the infinite seabed, in this study, the periodical boundary condition is applied to the left and right lateral boundaries in the consolidation computation:

$$\begin{aligned} u_s|_{x=80} &= u_s|_{x=330}, \\ v_s|_{x=80} &= v_s|_{x=330}, \\ w_s|_{x=80} &= w_s|_{x=330}, \\ p_s|_{x=80} &= p_s|_{x=330}. \end{aligned} \tag{9}$$

It means that the displacements and pore pressure on the left and right lateral sides of seabed are equal to each other at any time.

Third, the seabed and caisson breakwater under the static water level (SWL) are all applied by the hydrostatic pressure (Figure 2). Therefore, the surface of seabed and the outer surface of caisson breakwater are applied by the hydrostatic pressure which could be expressed as

$$p = \rho_f g(h + d - z), \tag{10}$$

where h is the thickness of seabed, d is the water depth, z is the vertical coordinate. The hydrostatic pressure acting on seabed and the caisson breakwater is perpendicular to the surfaces of seabed and caisson breakwater (Figure 2). Additionally, the pore pressure at seabed surface and the outer surfaces of caisson breakwater must be equal to the corresponding hydrostatic pressure to satisfy the continuity condition of water pressure at the interfaces.

On the part of caisson breakwater over the SWL, there is no force applying, and the water pressure is 0.

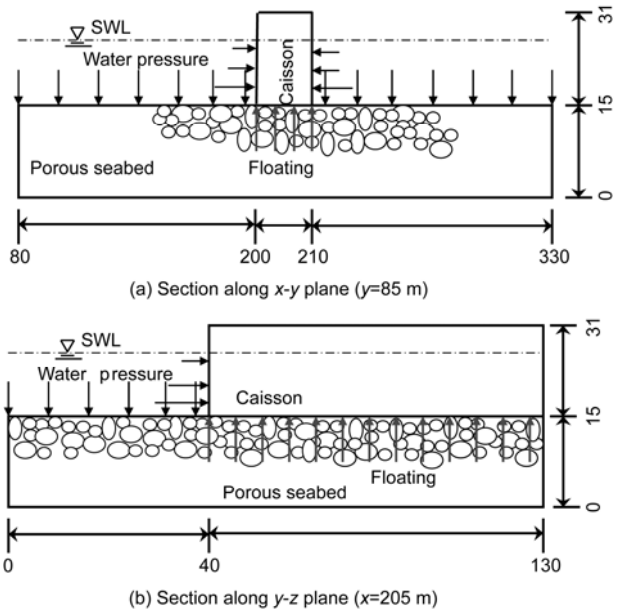

Figure 2 Schematic graph of the hydrostatic pressure and floating force acting on seabed surface and rigid caisson.

Fourth, the caisson breakwater is made of reinforcement concrete. Therefore, it is rigid and impermeable block. The caisson not only is applied by the hydrostatic pressure on lateral sides, but also is applied by the floating force on the bottom (see Figure 2). In this study, this floating force acting on the bottom of impermeable caisson is taken into consideration in computation. The magnitude is $\rho_f g d$; and the applying direction is upward.

3 Verification of 3D FEM soil model

In this study, a 3D FEM program (part of PORO-WSSI 3D) is developed, and adopted to solve the above boundary value problem. The PORO-WSSI 3D model is developed to investigate the interaction between wave, seabed and structures. Two sub-models (wave model and soil model) are included in PORO-WSSI 3D. The wave model is based on the Navier-Stokes equations, and solved by FVM. The soil model is based on the "u-p" approximation, and solved by FEM. An exchange port is developed to couple the two sub-models together. The soil model in PORO-WSSI 3D is developed based on the DYNE3WAC proposed by Ou (2009) [23]. And a new loading system is developed to replace the old loading system in DYNE3WAC which only could be applied to some simple loadings. The new loading system developed can deal with loading on arbitrary planes at arbitrary directions in 3D space. The finite element formulations of soil model can be found in Ye and Jeng (2011) [24].

In this section, the developed soil model is verified by an analytical solution proposed by Wang (2000) [25]. The computational domain is shown in Figure 3. There is a fully saturated sand layer with infinite lateral length applied by a constant uniform force P on the surface. The bottom of the sand layer is fixed and impermeable; however, the surface of the sand layer is permeable. Under the applying of uniform force P, the sand layer will be compressed and consolidated. The excess pore pressure will dissipate gradually. The property of the sand layer is assumed as: E=10^8 Pa, v=0.25, k=10^{-5} m s^{-1}. The thickness of the sand layer is h=20 m; and the length of computational domain in both x and y directions is chosen as 200 m. The uniform force is P=10 kPa. In order to simulate the infinite lateral length of sand layer, the periodical boundary condition is applied to the two lateral sides of the computational domain. The front and back boundaries are both fixed at y direction.

Figures 4 and 5 show the comparison of pore pressure and vertical displacement along the x=0 between the numerical results determined by PORO-WSSI 3D and the analytical solution proposed by Wang (2000) [25]. It can be seen that the numerical results agree very well with the analytical solution. Figure 6 shows the comparison of the settlement of the surface of sand layer between the numerical results and analytical solution. From Figure 6, it is found

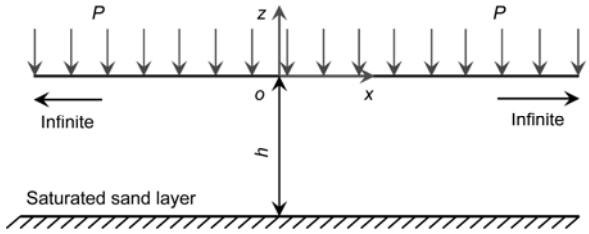

Figure 3 A saturated sand layer with infinite lateral length is applied by a constant force *P*.

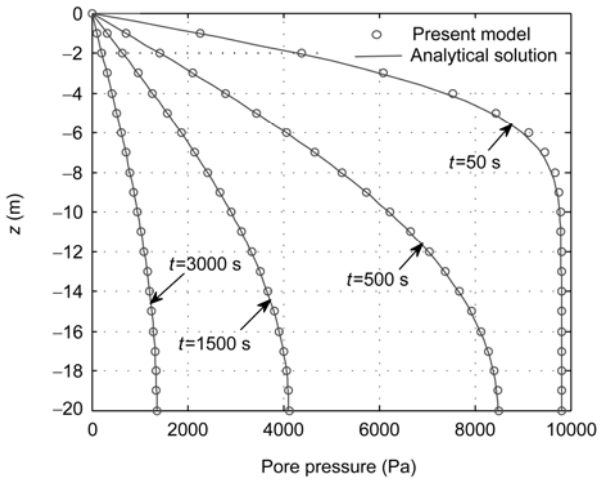

Figure 4 Comparison of pore pressure along x=0 between the numerical results and analytical solution at different times.

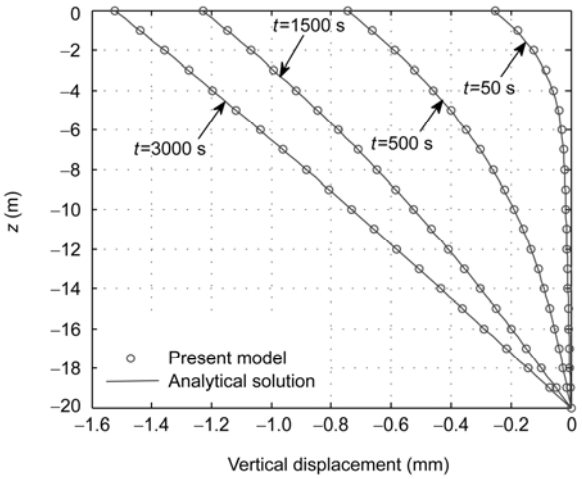

Figure 5 Comparison of vertical displacement along x=0 between the numerical results and analytical solution at different times.

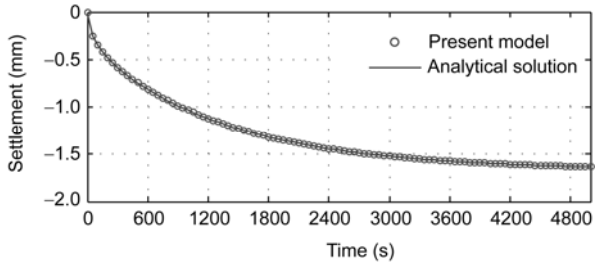

Figure 6 Comparison of the settlement of the surface applied by the constant force *P* between the numerical results and analytical solution.

that the numerical results determined by PORO-WSSI 3D are nearly perfectly consistent with analytical solution. All the consistency shown in Figures 4–6 proves that the soil model in PORO-WSSI 3D is reliable.

4 Results and discussion

In this section, the developed FEM program PORO-WSSI 3D is adopted to investigate the consolidation of 3D unsaturated seabed under a rigid caisson breakwater. The computational domain and the configuration of seabed and caisson breakwater are shown in Figure 1. The 27-nodes 3D brick isoparametric element is used to discretize the seabed and caisson breakwater. Due to the fact that it is the third order isoparametric element, the numerical results deserve high accuracy. The properties of seabed and caisson breakwater used in simulation are listed in Table 1. The water depth on seabed foundation is 10 m.

4.1 Consolidation process

It is well known that the seabed generally has experienced the consolidation process under the hydrostatic pressure and the self-gravity in the geological history. There is no excess pore pressure in seabed. In engineering, after the construction of a caisson breakwater on seabed, the weight of breakwater is initially transferred to the pore water in seabed foundation, resulting in the generation of excess pore pressure and pressure gradient. As time passing by, the pore water permeates driven by the pressure gradient through the void of soil particles, promoting the pore pressure to dissipate gradually (see Figure 7, t=4000 s and Figure 8(a)). From the distribution of pore pressure on section y=85 m, it is found that the pore pressure under the caisson breakwater is obviously greater than that of other position far away from the breakwater; and the maximum pore pressure is 280 kPa. In the consolidation process, the weight of breakwater gradually is transferred from the pore water to the soil particles (see Figure 8(b)); and the breakwater subsides correspondingly (see Figure 8(c)). Finally, the seabed foundation reaches a new equilibrium status, in which the excess pore pressure and pressure gradients disappear (see Figure 7, t=40000 s). The maximum pore pressure in seabed has decreased from 280 kPa to 220 kPa. It is noted that the pore pressure in the rigid caisson breakwater is zero at any time due to that it is impermeable. This newly reached consolidation status should be taken as the initial status for the

Table 1 Properties of seabed, and caisson breakwater used in simulation

Medium	ϕ (°)	E (MPa)	ν	k (m s^{-1})	S_r (%)	n	G_s
Seabed	35	20	0.33	10^{-5}	98	0.25	2.65
Caisson	45	10000	0.25	0	0	0	2.65

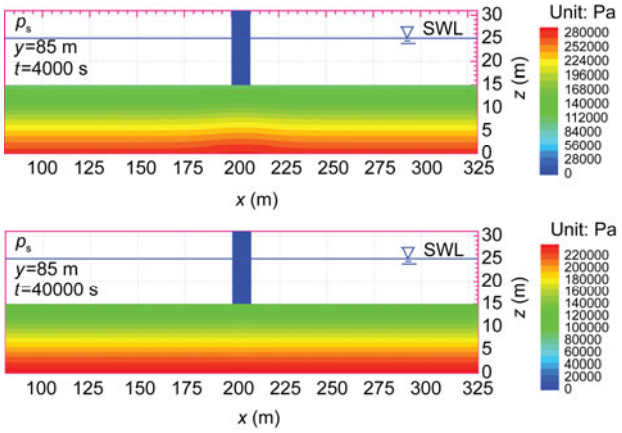

Figure 7 Distribution of pore pressure on section x=85m in seabed and caisson at time 4000 s and 40000 s.

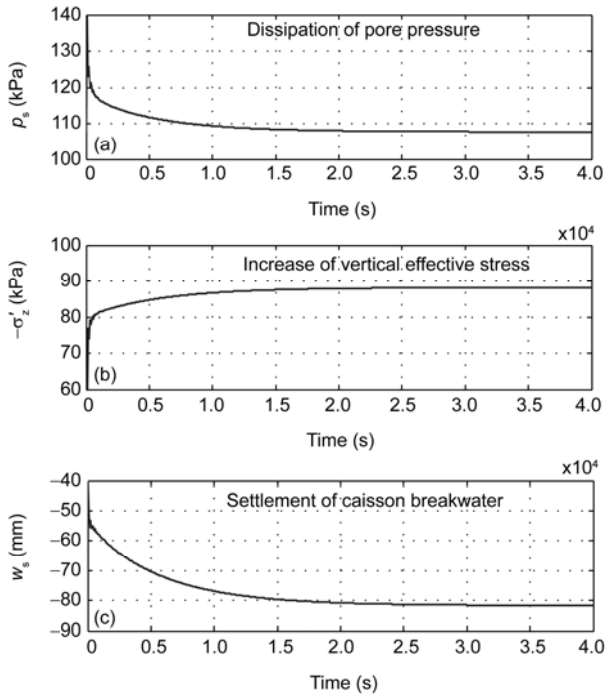

Figure 8 Historic curve in consolidation process for the dissipation of pore pressure, increase of effective stress at position (x=205 m, y=85 m, z=6 m) and the settlement of caisson breakwater.

evaluation of the dynamic response of seabed foundation and breakwater under ocean wave/earthquake loading.

In the process of consolidation, part of pore water in porous seabed will flows out of seabed through the seabed surface, to provide sand particles with enough space to be compacted. Figure 9 demonstrates the flux of pore water flowing out of seabed at position (x=176 m, y=85 m, z=15 m). As illustrated in Figure 9, the flowing out flux is great at the initial stage; however, there is basically no pore water flowing out at the later stage of consolidation process.

4.2 Effect of floating force

In the offshore environment, the caisson breakwater generally is made of reinforcement concrete, which is nearly rigid and impermeable comparing with sandy bed. The bottom of caisson is acted by an upward floating force. Consideration of this upward floating force acting on the bottom of caisson in calculation is very important to accurately determine the stress, displacement field and the final settlement of caisson. Undoubtedly, the effective stresses, vertical displacement in seabed foundation and the final settlement of caisson will be overestimated greatly if the upward floating force is not applied to the bottom of caisson. This conclusion can be observed clearly from Figure 10. The vertical effective stress on line (y=85 m, z=10.5 m) and the vertical displacement on line (y=85 m, z=15 m) under the caisson breakwater is about two times of that if the floating force is not applied in calculation. Therefore, the floating force acting on the bottom of caisson cannot be ignored.

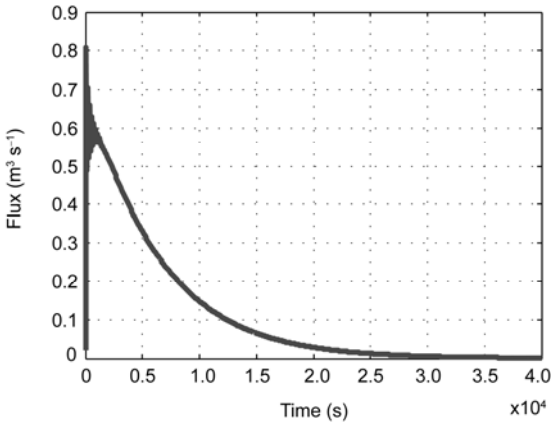

Figure 9 Upward flux of pore water at positions (x=176 m, y=85 m, z=15 m) in the process of consolidation.

4.3 Distribution of stresses fields

In engineering, it is necessary for designers to know how the stresses are distributed in seabed foundation under marine structures after the consolidation process is completed. In this section, the distribution of stresses in seabed foundation under the caisson breakwater and hydrostatic pressure loading are investigated intensively. Two typical sections (y=85 m and x=205 m) in seabed foundation are chosen to demonstrate the distribution of stresses.

Figures 11 and 12 show the distribution of effective stresses σ'_x, σ'_y and σ'_z on the two typical planes. As illustrated in Figures 11 and 12, the effect of the caisson breakwater on the stresses field is significant. The effective stresses all increase significantly in the zone under or near to the caisson breakwater due to the gravity induced compression. However, the effect of marine structures on stress field in seabed foundation will basically disappear in the zone far away from the marine structures; and the distribution of effective stresses is layered, which is nearly the same with that when there is no marine structure on seabed.

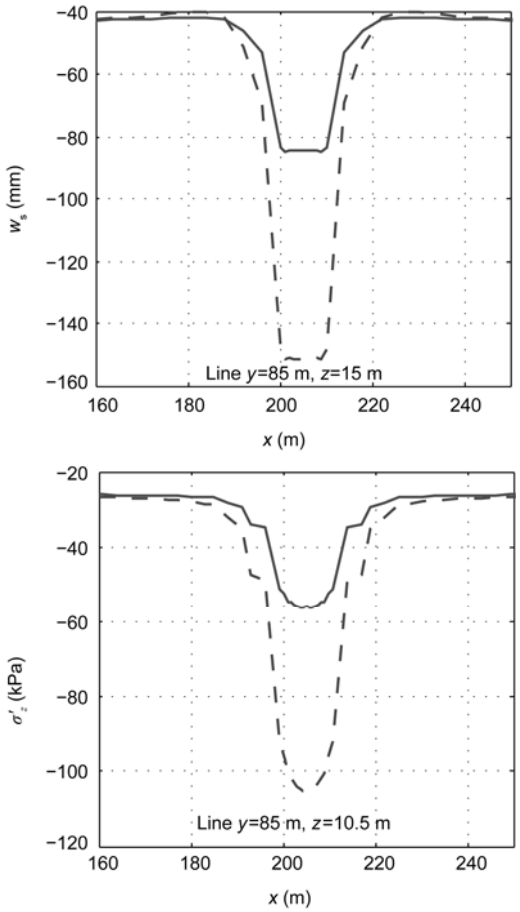

Figure 10 Distribution of vertical displacement on line (y=85 m, z=15 m) and vertical effective stress on line (y=85 m, z=10.5 m). Solid line: floating force is applied; dotted line: floating force is not applied.

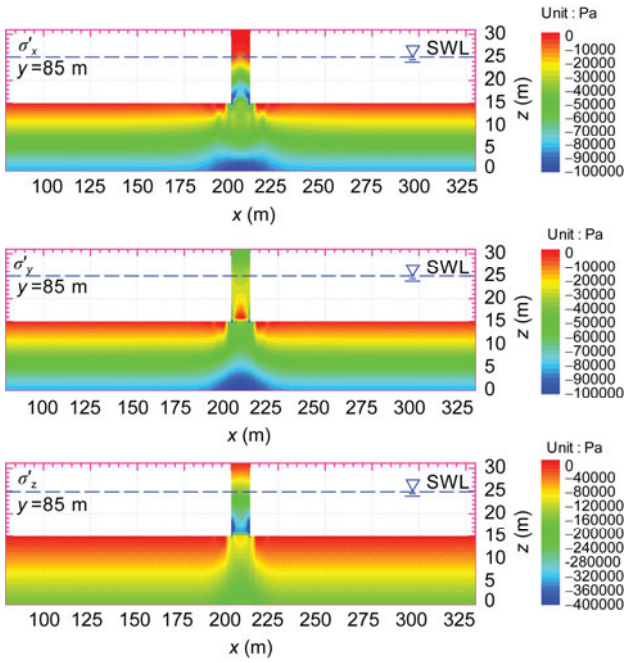

Figure 11 Distribution of effective stresses on section y=85 m.

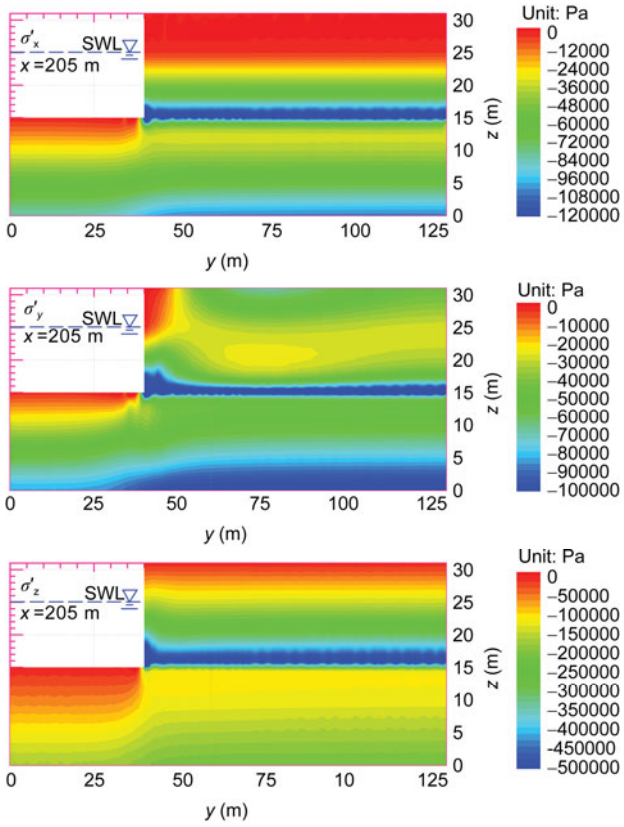

Figure 12 Distribution of effective stresses on section x=205 m.

From Figure 12, it is found that there is a concentration zone of compression stress in the bottom of caisson breakwater. This could attribute to that the bottom of caisson breakwater is applied by a huge upward floating force (about 98 kPa) induced by the hydrostatic pressure. Due to the fact that the caisson breakwater is much stiffer than that of seabed foundation, the caisson breakwater behaves like a rigid object. The failure could not occur in the caisson breakwater. Therefore, the stresses in caisson breakwater are not the investigating content in this study.

Figures 13 and 14 demonstrate the distribution of shear stresses in seabed foundation on section y=85 m and x=209 m. Here, the symmetric plane x=205 m is not chosen due to that the τ_{xy} and τ_{xz} are zero on the symmetric plane. The distribution of τ_{xy} and τ_{xz} on x=209 m can be observed more clearly. From Figures 13 and 14, it can be seen that the concentration zone of shear stress only locates in the region under or near to the caisson breakwater. In the region far away from the caisson breakwater, there is no shear stress. It is indicated that the construction of marine structures on seabed is the direct reason for the shear stress concentration in foundation. The τ_{xy} and τ_{yz} only exist in the zone under or near to the head of breakwater in the seabed. The magnitude of τ_{xy} is small (maximum 5 kPa), However, the τ_{zy} is a little large, up to 20 kPa. Differently, the τ_{xz} is distributed in the whole zone under the caisson breakwater; and the magnitude

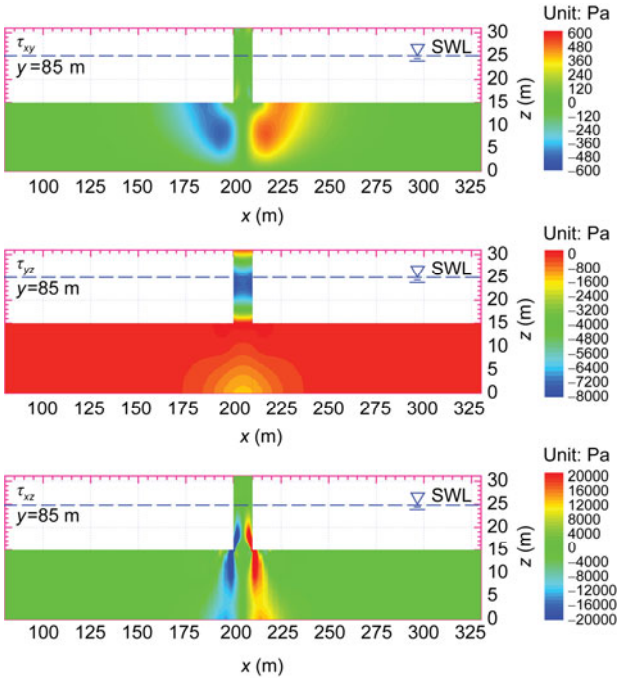

Figure 13 Distribution of shear stresses on section y=85 m.

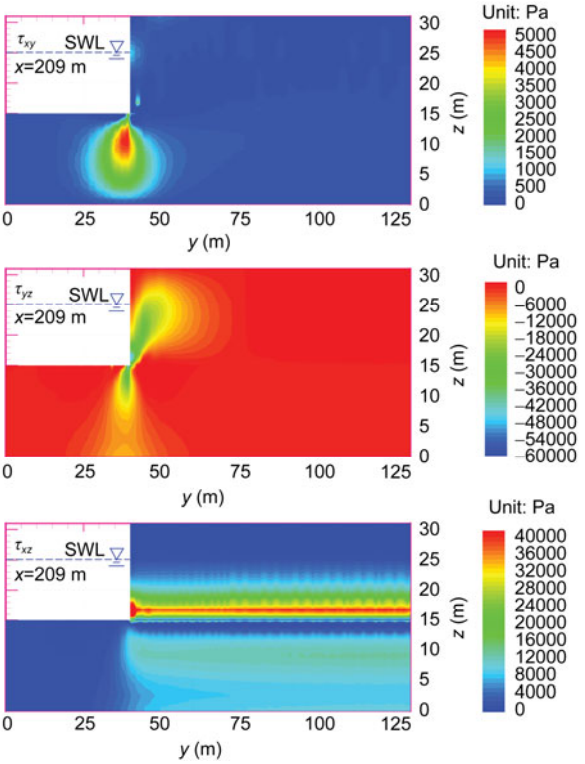

Figure 14 Distribution of shear stresses on section x=209 m.

could reach up to 70 kPa. Therefore, the τ_{yz} and τ_{xz} should be responsible for the shear failure of seabed foundation under marine structures. In engineering practice, the coastal engineers should pay their attention to the τ_{yz} and τ_{xz} developed in seabed foundation due to the gravity loading of marine structures.

4.4 Distribution of displacement fields

In offshore engineering, the final settlement of marine structures built on seabed should be controlled. Excessive settlement due to the heavy structure and/or soft seabed foundation is not acceptable from the view of engineering safety and people's psychology. Therefore, it is important for engineering designers to predict and evaluate the displacement fields in seabed foundation under marine structures. The developed FEM program PORO-WSSI 3D is applicable to the determination of the displacement fields in seabed foundation and the settlement of marine structures.

Figures 15 and 16 illustrate the distribution of displacements u_s, v_s and w_s in seabed foundation on the two typical sections y=85 m and x=205 m. From Figures 15 and 16, it is found that the seabed foundation moves toward the two lateral sides, $-y$ direction and the bottom of seabed under the compression of caisson breakwater. The deformation of seabed mainly occurs in the zone under the caisson breakwater. The maximum displacement in x and y directions is 8 and 6 mm respectively. The maximum displacement of v_s is located at the point under the head of caisson breakwater. Due to the compressive deformation of seabed foundation, the caisson breakwater subsides downward. The final settlement of caisson breakwater is about 81.7 mm. The horizontal displacement u_s on section x=205 m is near zero because this plane is the symmetric plane of computational domain. Under the loading of hydrostatic pressure and self-weight of soil, the seabed far away from the caisson breakwater also subsides; the final settlement is about

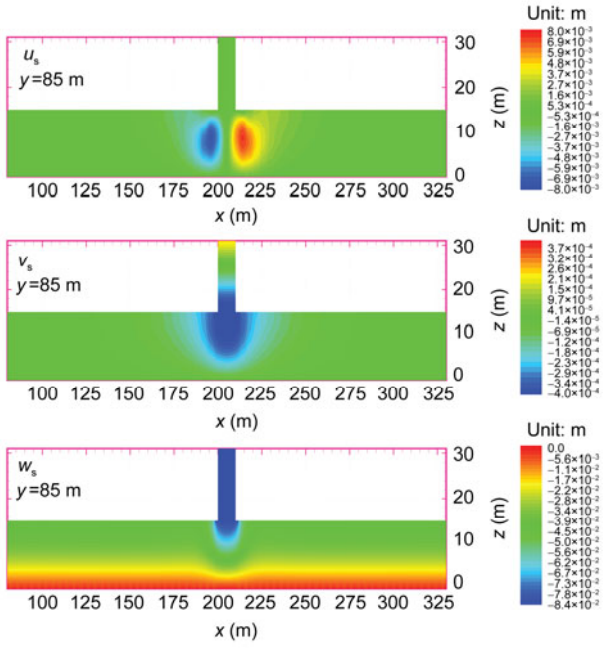

Figure 15 Distribution of displacements on section y=85 m.

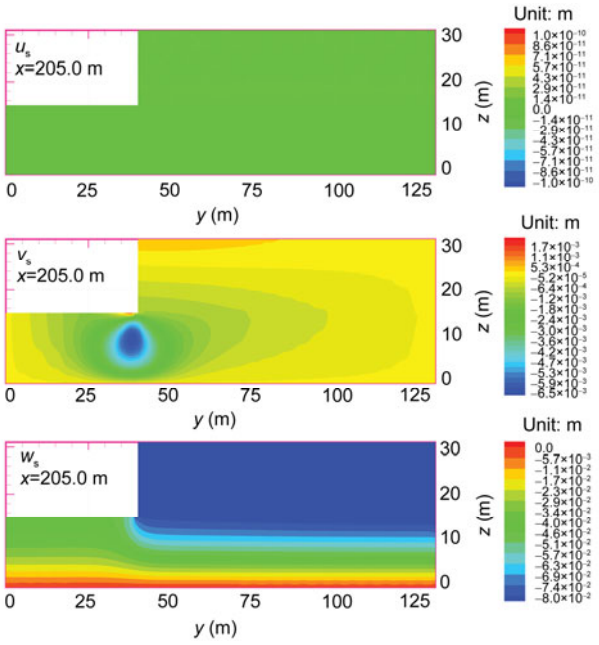

Figure 16 Distribution of displacements on section x=205 m.

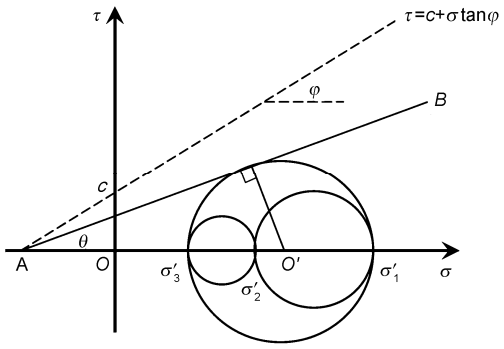

Figure 17 The Mohr-Coulomb criterion.

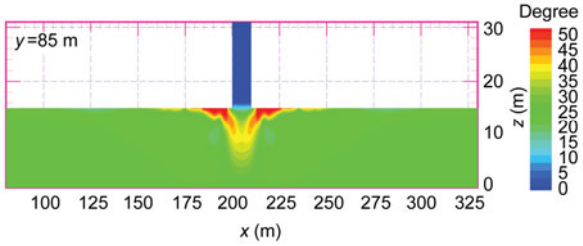

Figure 18 Distribution of stress angle on section y=85 m.

40 mm. Here, it is noted that the displacements in seabed and the settlement of marine structures mainly depend on the Young's modulus of seabed foundation.

4.5 Prediction of shear failure in seabed foundation

In offshore engineering, it is important for coastal engineers involved in the design of a breakwater to predict the instability of seabed foundation due to shear failure. In the study, the developed FEM program PORO-WSSI 3D could provide the coastal engineers with a powerful analysis tool to evaluate the potential instability of seabed foundation due to shear failure under the marine structures loading, such as breakwater, pipeline, turbine and oil platform.

The Mohr-Coulomb criterion is widely used to judge the occurrence of shear failure in seabed foundation in offshore engineering. In Figure 17, if the angle θ (known as stress angle) of the tangent AB of a maximum Mohr circle is greater than or equal to the friction angle ϕ of sandy seabed foundation, the shear failure occurs at this point:

$$\theta = \arcsin\left(\frac{\dfrac{\sigma_1' - \sigma_3'}{2}}{\dfrac{c}{\tan\phi} + \dfrac{\sigma_1' + \sigma_3'}{2}}\right) \geqslant \phi, \tag{11}$$

where c and ϕ are the cohesion and friction angle of sand soil; σ'_1 and σ'_3 are the maximum and minimum principal effective stresses.

Figure 18 illustrates the distribution of stress angle in seabed foundation on the section y=85 m. It is observed that the stress angle in the region near to the caisson breakwater is generally greater than that in other region far away from the breakwater. It is indicated that the construction of caisson breakwater on seabed has significant effect on the stress field in seabed foundation. In the seabed foundation under the caisson breakwater, there are zones in which the shear failure occurs according to the Mohr-Coulomb criterion. Figure 19 shows the isosurfaces of stress angle θ=35° in the seabed foundation under the caisson breakwater. In Figure 19, it can be found that there are two isosurfaces. The region between the two isosurfaces (θ=35°) is the predicted shear failure zone in seabed foundation. In the zone between the bottom of caisson breakwater and the small size isosurface (θ=35°), there is no shear failure. The sandy soil behaves like a rigid object in this zone. Figure 20 demonstrates the predicted shear failure zone in seabed foundation on section y=85 m and symmetric plane x=205 m. From Figure 20, we can easily find the predicted shear failure zone and the rigid wedge under the caisson breakwater. According to the numerical results determined by PORO-WSSI 3D, the shear failure induced instability in the seabed foundation with the properties listed in Table 1 is expected to occur. In offshore engineering, if the shear failure instability is predicted to occur, some engineering methods, such as replacement of the weak seabed soil, have to be adopted to avoid the occurrence of instability of foundation.

4.6 Effect of seabed properties and water depth

In practical engineering, the porous seabed chosen as the

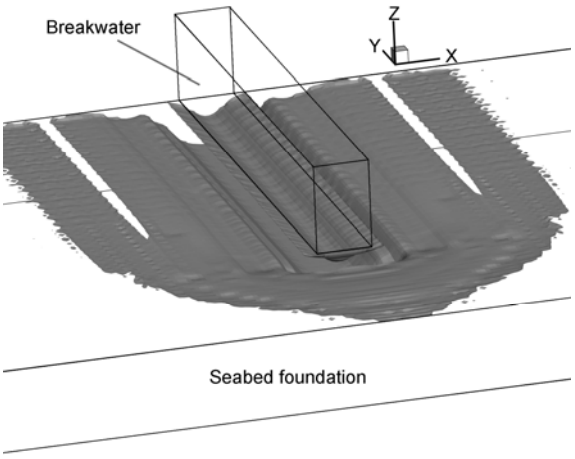

Figure 19 Isosurfaces (θ=35°) of stress angle in seabed foundation.

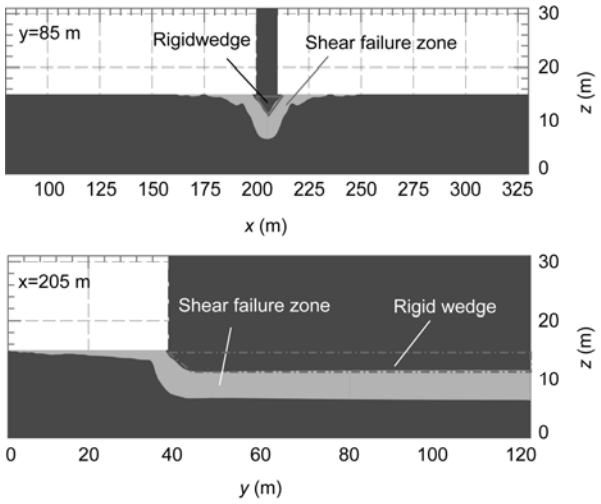

Figure 20 The predicted shear failure zone in seabed foundation.

foundation of marine structures is different from case to case. It results in that the property parameters of seabed foundation are various. How the seabed properties and water depth affect the final consolidation status is a problem for coastal engineers. In designing work, what the coastal engineers most concern includes two aspects: (1) whether the final settlement of marine structures is acceptable; (2) whether the shear failure would occur in the seabed foundation under marine structures. In this section, the final settlement of caisson breakwater, and the shear stress τ_{xz} at position (x=199.1 m, y=85 m, z=10.5 m) are taken as the representative values to investigate the effect of seabed properties and water depth.

Table 2 lists the results of the final settlement of caisson breakwater and the shear stress τ_{xz} under different conditions. From the results listed in Table 2, it is found that the shear stress τ_{xz} basically is not affected by the Young's modulus E, permeability k, saturation S_r and the water depth d. The final settlement of caisson breakwater is significantly affected only by the Young's modulus E. Other parameters, such as k, S_r and d also have no effect on the final consolidation status of seabed foundation under marine structures. In practical engineering, the porous seabed with high Young's modulus and bearing capacity should be chosen as the foundation of marine structures.

5 Dynamics of seabed foundation and caisson breakwater under ocean wave loading

In offshore area, the breakwaters built on porous seabed are inevitably attacked by the environmental loading—the ocean wave. Under this kind of circle loading, the breakwater would lose its stability due to the excess dynamic shear stress and the liquefaction of the seabed foundation. In engineering history, some examples of the instability of breakwater in offshore environment due to the ocean wave loading have been reported in refs. [3, 26–28]. The investigation of the interaction between the ocean wave, breakwater and its foundation is necessary and meaningful in practical engineering. In this section, the dynamics of seabed foundation and caisson breakwater under ocean wave loading is briefly studied by adopting the developed 3D coupled numerical model PORO-WSSI 3D.

5.1 3D wave loading

When studying the interaction mechanism between the ocean wave, marine structure and seabed foundation, the ocean wave induced dynamic pressure acting on seabed surface and marine structure is the key problem. In most previous investigations [29–31], the analytical solutions of wave induced pressure are used due to that there is no

Table 2 Final settlement of caisson and the shear stress at (x=199.1 m, y=85 m, z=10.5 m) under different seabed conditions

Item	Result		Item	Result		Item	Result		Item	Result	
E (MPa)	w_s (mm)	τ_{xz} (kPa)	k (mm s^{-1})	w_s (mm)	τ_{xz} (kPa)	S_r (%)	w_s (mm)	τ_{xz} (kPa)	d (m)	w_s (mm)	τ_{xz} (kPa)
10	163.2	24.1	0.0001	81.6	24.3	95	81.5	24.2	8	81.7	24.3
20	81.7	24.3	0.01	81.7	24.3	98	81.7	24.3	10	81.7	24.3
60	21.1	24.5	1.0	81.7	24.5	100	81.6	24.1	12	81.7	24.4

Note: The standard parameters are E=20 MPa, k=0.01 mm s^{-1}, S_r=98%, d=10 m. When studying the effect of one of these parameters, other parameters are kept the same with standard parameters.

marine structure or simplified structures (without width or with simple outer shape). For complicated marine structures, the analytical solution generally is not available. In the developed coupled numerical model PORO-WSSI 3D, the wave induced dynamic pressure acting on seabed and marine structures is determined by numerically solving the Navier-Stokes equations with FVM. The detailed description of this model will be further presented in the future publication.

Adopting the coupled numerical model PORO-WSSI 3D, the ocean wave around the caisson breakwater is determined by solving Navier-Stokes equations with FVM. The wave characteristics used here are: wave height H=1.5 m, wave period T=8.0 s, and water depth d=10 m. The mass source functions being attached to the mass continuity equation is adopted to generate the target wave train like that in ref. [32]. The numerical configuration for wave field generation is shown in Figure 21. Three absorbing zones are set to dissipate the unexpectedly reflected wave due to the limited computation domain size.

Figure 21 illustrates the wave profile around the caisson breakwater at two typical times t=60 s and t=64 s. At time t=60 s, the wave trough arrives at the breakwater; at time t=64 s, the wave crest arrives at the breakwater. As illustrated in Figure 21, there are three zones around the breakwater in which the waves are significantly different. In front of the caisson breakwater, the wave is highly similar to the standing wave due to the interference between the incident wave and reflected wave. The wave height in this zone is basically 3.0 m which is nearly two times of the original wave height at the wave maker. Behind the caisson breakwater, the wave is diffracted wave due to the diffraction effect. The wave height behind the breakwater is much smaller than the original wave height (H=1.5 m). In the other zone, the wave is progressive wave; the wave height basically keeps the same with the original wave height.

The wave field around the caisson breakwater, including the velocities and the water pressure (hydrostatic plus dynamic pressure) in the whole computational domain can be completely determined adopting the 3D wave model in PORO-WSSI 3D. Then, the water pressure is applied to the seabed and caisson breakwater. The dynamic response of breakwater and seabed foundation can be determined by the 3D soil model in PORO-WSSI 3D.

5.2 Dynamic response of caisson breakwater

As mentioned in the previous section, the initial status of seabed foundation for the dynamic response analysis under wave loading should be the final consolidation status under hydrostatic pressure, weight of breakwater and self-gravity, rather than assuming all the physical quantities, such as displacements, stresses, are all zero. In this section, taking the final consolidation status determined in Section 4 for the breakwater and seabed foundation system as the initial condition, the dynamics of caisson breakwater and its seabed foundation is investigated.

During the interaction between the ocean wave and caisson breakwater, the wave trough and wave crest periodically arrive at the breakwater, and collide with the caisson breakwater. The impact force acting on the front lateral side also vibrates accordingly (Figure 22). This periodical impact force on breakwater makes the breakwater move forward and backward periodically (Figure 23). It is found from Figure 22 that the diffracted wave induced dynamic pressure on the behind lateral side of breakwater is apparently relatively smaller than that on the front lateral side. It is indicated that the breakwater indeed is effective to block the wave, and dissipate the wave energy.

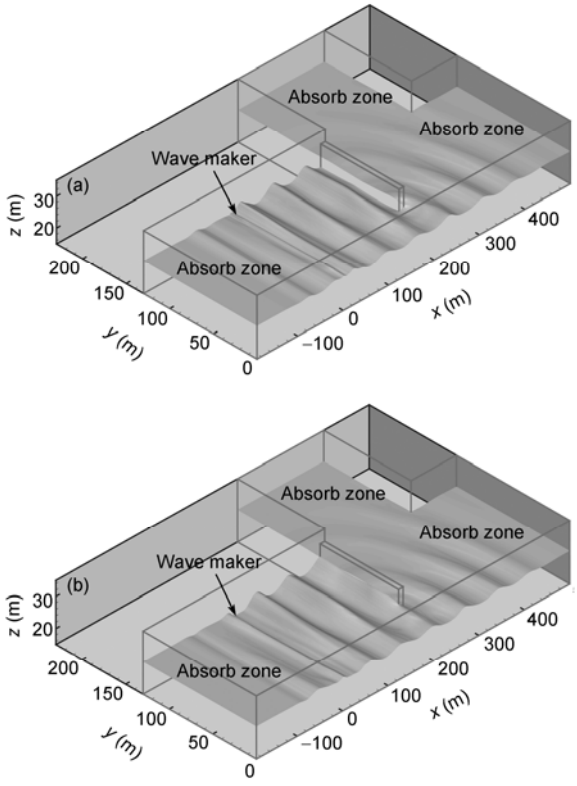

Figure 21 3D wave profile at two typical times t=60 s and t=64 s around the caisson breakwater. (a) t=60 s (wave trough arriving at breakwater); (b) t=64 s (wave crest arriving at breakwater).

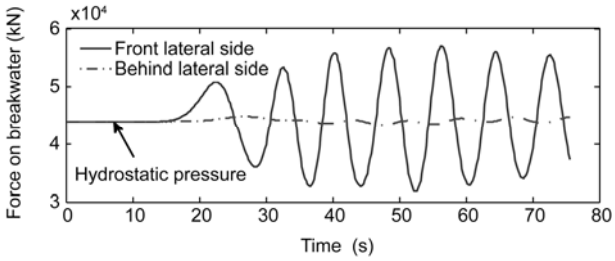

Figure 22 Total wave impact force acting on the front and behind lateral sides of caisson breakwater (hydrostatic plus wave induced pressure).

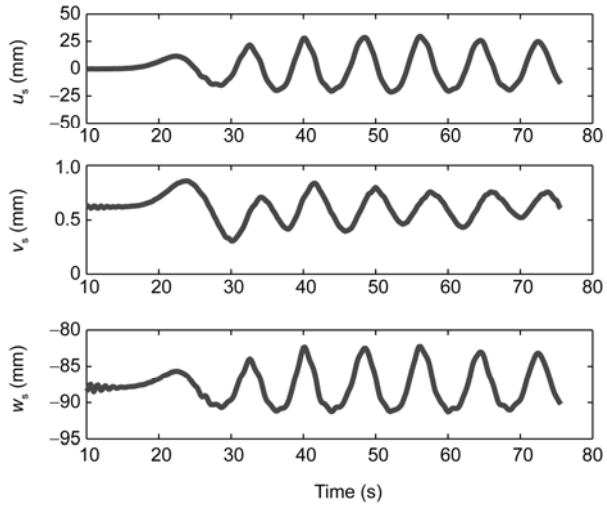

Figure 23 Wave induced displacements of caisson breakwater under the ocean wave loading.

5.3 Dynamic response of seabed foundation

Under the 3D wave loading, the seabed foundation also has corresponding response to the wave. Figure 24 shows the hydrostatic and wave induced water pressure acting on the seabed at three typical positions. They are in front of breakwater (x=180 m, y=85 m, z=15 m), behind breakwater (x=230 m, y=85 m, z=15 m) and near to the breakwater head (x=205 m, y=20 m, z=15 m). It also can be seen that wave induced pressure acting on seabed foundation behind the breakwater is much smaller than that in other two typical positions. The wave induced pressure in front of breakwater is the greatest due to the interference between incident wave and reflected wave; and the nonlinearity is clear. Correspondingly, the wave induced pore pressure in seabed foundation is also significantly different in the three typical positions (Figure 25). From Figure 25, it is found that the seabed's response is the strongest in front of the breakwater; and it is the weakest behind the breakwater.

Figures 26 and 27 illustrate the 3D wave induced dynamic response in seabed foundation at typical time t=60 s

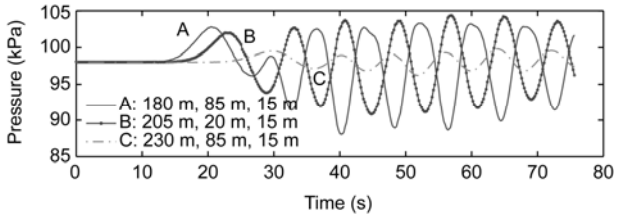

Figure 24 Water pressure (hydrostatic plus wave induced) acting on the seabed at three typical positions: in front of breakwater, behind breakwater and near to the breakwater head.

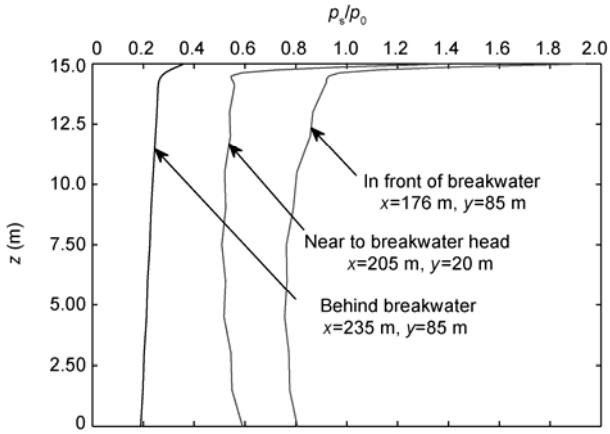

Figure 25 Vertical distribution of the maximum wave induced pore pressure in seabed foundation at three typical positions ($p_0=\gamma_w H/2\cosh(\lambda d)$, λ is the wave number).

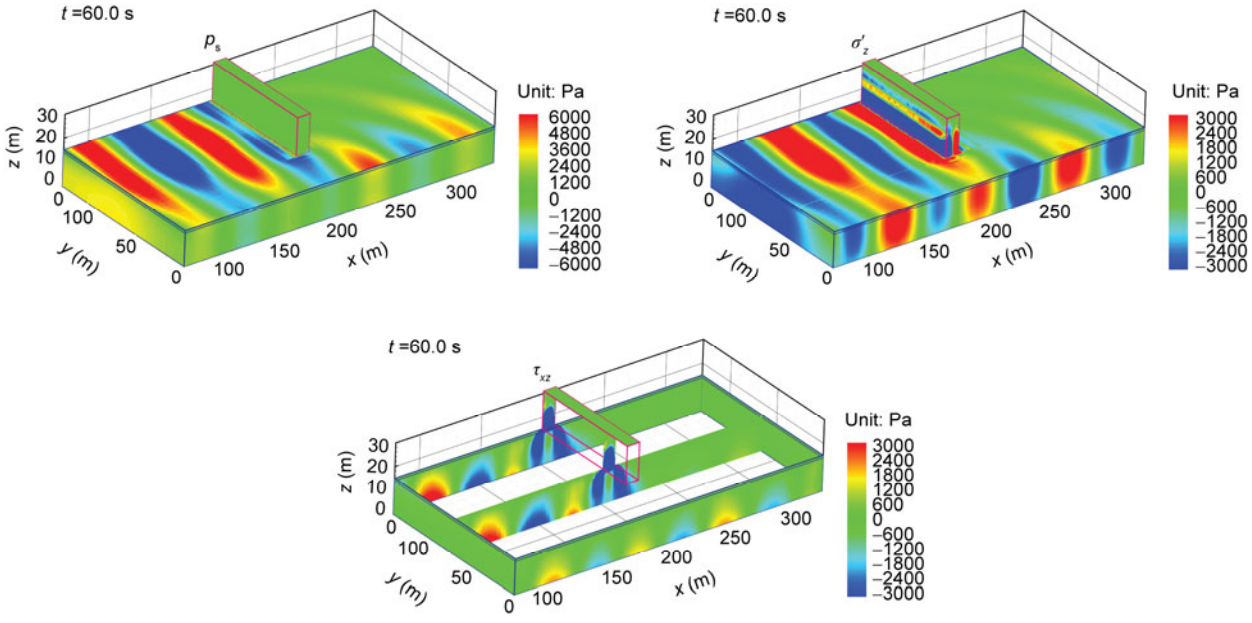

Figure 26 Wave induced dynamic response in seabed foundation at time t=60 s.

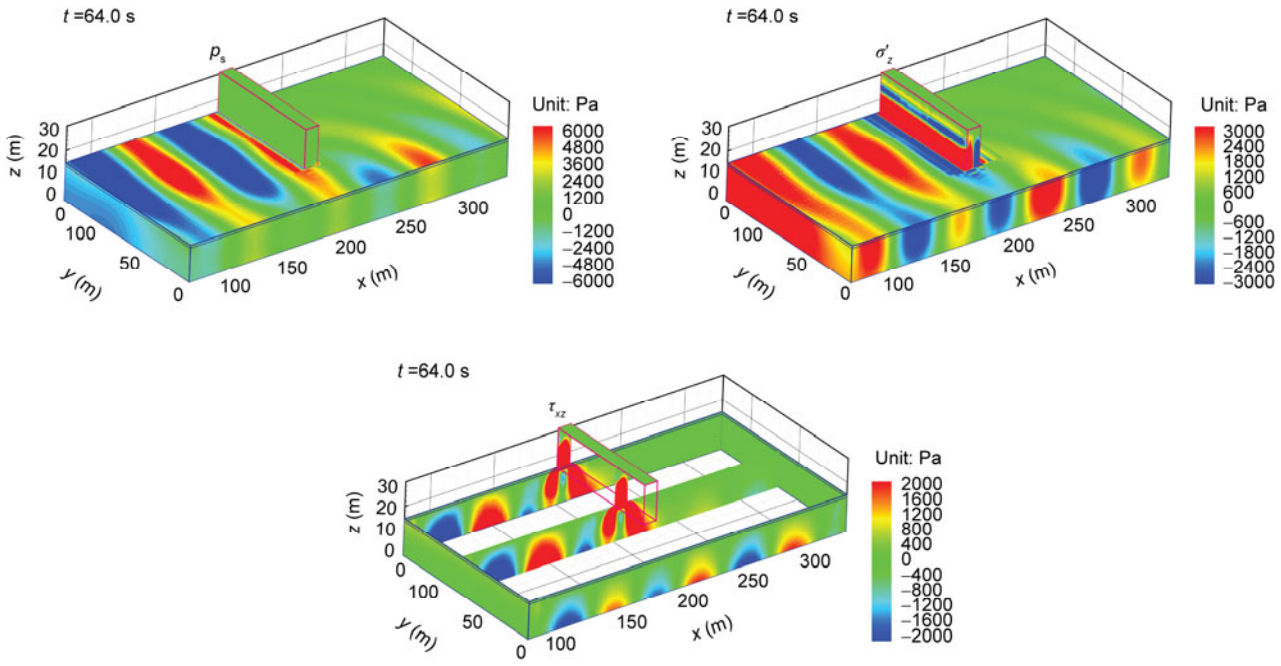

Figure 27 Wave induced dynamic response in seabed foundation at time t=64 s.

and t=64 s taking the pore pressure p_s, vertical effective stress and shear stress τ_{xz} as the representative physical quantities. Due to the fact that the 3D wave propagating around the caisson breakwater owns periodicity, the response of seabed foundation to it also is periodical. From Figures 26 and 27, it is easy to find again that the response of seabed foundation in front of the breakwater is the strongest; and the response of seabed behind the breakwater is the weakest. It is indicated that the breakwater can effectively block the wave in the offshore environment. There are concentrated zones of the wave induced dynamic shear stress τ_{xz} under the caisson breakwater. And the direction of the concentrated dynamic shear stress τ_{xz} changes periodically under the wave loading. Then the cycle shear loading is formed in the zone under the caisson breakwater. The magnitude of the cycle dynamic shear stress τ_{xz} could reach up to 10 kPa. This is a very harmful factor for the caisson breakwater to keep its stability on seabed due to that the dynamic shear failure would occur. As illustrated in Figures 26 and 27, under the wave crest, the wave induced pore pressure in seabed foundation is positive, and the dynamic vertical effective stress is compressive. The seepage force is also downward. Therefore, the seabed under wave crest is impossible to be liquefied. While, under the wave trough, the wave induced pore pressure is negative; and the dynamic vertical effective stress is tensile. The seepage force is upward. If the upward seepage force could overcome the overburdened soil weight in some zones, then the soil in these zones will be liquefied transiently.

Figures 28 and 29 demonstrate the predicted wave

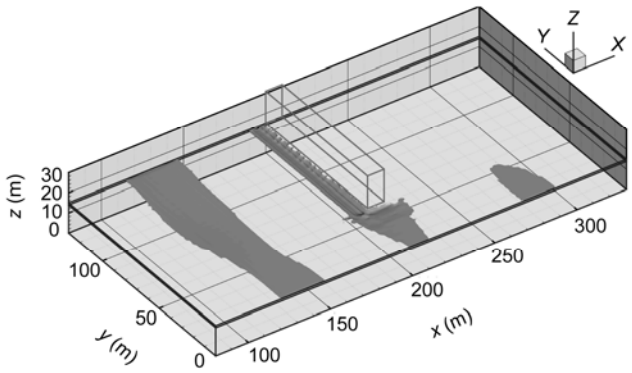

Figure 28 The predicted wave induced liquefaction zone in seabed at time t=60 s.

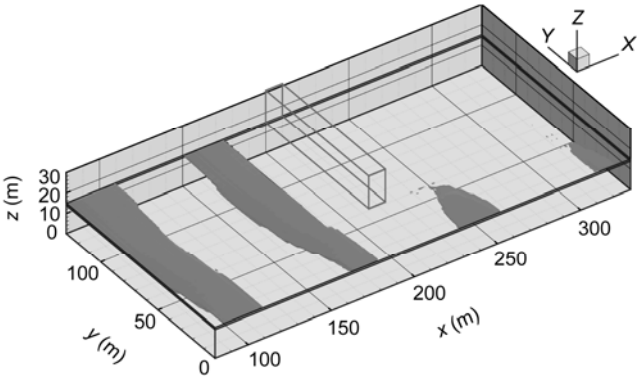

Figure 29 The predicted wave induced liquefaction zone in seabed at time t=64 s.

induced liquefaction zones in seabed foundation at the two typical times t=60 s and t=64 s. Here, the liquefaction criterion proposed by Okusa (1985) [33] is used:

$$-(\sigma'_z)_{\text{initial}} \leqslant (\sigma'_z)_{\text{dynamic}}, \tag{12}$$

where $(\sigma'_z)_{\text{initial}}$ is the initial vertical effective stress in initial consolidation status, $(\sigma'_z)_{\text{dynamic}}$ is the wave induced vertical effective stress. The above liquefaction criterion is acceptable, and has been widely applied in refs. [29–32, 34, 35].

Figures 28 and 29 further prove that the seabed only could be liquefied under wave trough. At time t=60 s, the wave trough arrives at the breakwater, making the seabed foundation near to the caisson breakwater to be liquefied. This liquefaction would make the caisson breakwater tilt or collapse due to the fact that the liquefied sand behaves like a kind of liquid, which cannot support any marine structure. This phenomenon was also observed by Zhang (2009) [36] in a centrifuge test. However, this liquefied status of sand only could last for a while, when the wave crest arrives at the breakwater, this liquefied zone near to the caisson breakwater disappears (see Figure 29). Therefore, this liquefied zone near to breakwater appears periodically. The maximum liquefaction depth in this zone could reach up to 0.58 m. Another phenomenon observed from Figures 28 and 29 is that the seabed foundation behind the breakwater is not liquefied in all the time. The reason obviously is that the caisson breakwater has blocked the wave, and only the diffracted wave exists behind the breakwater.

6 Conclusions

In this study, a 3D coupled numerical model PORO-WSSI 3D is developed to investigate the interaction between the wave, seabed and marine structures. In PORO-WSSI 3D model, the soil model based on the dynamic Biot's equation (u-p formulation) is solved adopting FEM for space discretization, and Generalized Newmark-β method for time integration; and the wave model based on Navier-Stokes equations is solved adopting FVM. The soil model is validated by the analytical solution proposed by Wang (2000) [25]. By adopting PORO-WSSI 3D, the consolidation and dynamic response of 3D unsaturated seabed with a rigid caisson breakwater under ocean wave loading is investigated. Based on the analysis, following conclusions can be made:

(1) The floating force acting on the bottom of caisson breakwater has to be considered in calculation; otherwise, the effective stress and settlement of caisson breakwater will be overestimated.

(2) At initial stage of consolidation, the weight of marine structure is mainly supported by the pore water. As time passing by, the weight gradually is transmitted to soil particles, accompanying with the dissipation of excess pore pressure. The effective stresses increase significantly, and the shear stresses concentrate in the region under marine structures. In the region far away from the caisson breakwater, the effect of caisson breakwater disappears gradually.

(3) Under the compression of caisson breakwater, the seabed foundation moves toward two lateral sides, $-y$ direction and bottom of seabed. Correspondingly, the caisson breakwater subsides. The magnitude of displacement and the final settlement of marine structures mainly depend on the stiffness of seabed foundation.

(4) The developed 3D soil model is applicable to the prediction of the shear failure in seabed foundation. Under the conditions given in Table 2, it is predicted that the shear failure could occur in a large area in seabed.

(5) The parametrical study indicates that the shear stress in seabed foundation basically is not affected by the properties of seabed and water depth. The displacement field and the settlement of marine structures are significantly affected by the Young's modulus of seabed foundation. However, other parameters have no effect either on the displacement field in seabed foundation.

(6) There are three types of wave around the caisson breakwater: standing wave in front of breakwater, diffracted wave behind breakwater and progressive wave near to the breakwater head. The standing wave is the strongest wave, while the diffracted wave is the weakest wave. It results in that the seabed response in the three typical zones is significantly different. The seabed response in the zone in front of breakwater is much more intensive than that in the zone behind breakwater.

(7) Under the wave impact force loading, the caisson breakwater moves forward and backward periodically. There are two concentrated zones for the wave induced dynamic shear stress τ_{xz} in the seabed under the breakwater. This cycle wave induced shear stress is a harmful factor for the stability of breakwater due to probable shear failure.

(8) It is proved that the seabed foundation only could be liquefied transiently under the wave trough due to the fact that the upward seepage force in seabed can overcome the overburdened soil weight in some zones. In practical offshore environment, when the wave trough arrives at the breakwater, it is quiet possible for the breakwater to tilt or collapse due to the liquefaction of seabed foundation. Meanwhile, when the wave crest arrives at the breakwater, the breakwater could be overthrown by the wave impact force. Therefore, the above-mentioned two failure mechanisms both should be taken into consideration in engineering design.

The authors are grateful for the financial support from EPSRC #EP/G006482/1. The first author Ye Jianhong appreciates the funding support of Oversea Research Student Award from Scottish Government, UK.

1 Chung S G, Kim S K, Kang Y J, Im J C et al. Failure of a breakwater founded on a thick normally consolidated clay layer. Geotechnique, 2006, 56(3): 393–409
2 Franco L. Vertical breakwaters: the Italian experience. Coast Eng, 1994, 22(1-2): 31–55
3 Lundgren H, Lindhardt J H C, Romold C J. Stability of breakwaters on porous foundation. In: Proceeding of 12th International Conference on Soil Mechanics and Foundation Engineering, Rio de Janeiro, 1989. 451–454
4 Yamamoto T, Koning H, Sellmeijer H, et al. On the response of a poro-elastic bed to water waves. J Fluid Mech, 1978, 87(1): 193–206
5 Hsu J R, Jeng D S. Wave-induced soil response in an unsaturated anisotropic seabed of finite thickness. Int J Num Anal Meth Geomech, 1994, 18(11): 785–807
6 Ulker M B C, Rahman M S, Jeng D-S. Wave-induced response of seabed: Various formulations and their applicability. Appl Ocean Res, 2009, 31(1): 12–24
7 Jeng D S, Cha D H, Lin Y S et al. Wave-induced pore pressure around a composite breakwater. Ocean Eng, 2001, 28: 1413–1435
8 Mizutani N, Mostarfa A, Iwata K. Nonlinear regular wave, submerged breakwater and seabed dynamic interaction. Coast Eng, 1998, 33: 177–202
9 Mostafa A, Mizutani N, Iwata K. Nonlinear wave, composite breakwater, and seabed dynamic interaction. J Waterw, Port, Coast, Ocean Eng, 1999, 25(2): 88–97
10 Ye J H, Jeng D-S, Liu P L-F, et al. An integrated model for the wave induced seabed response around marine structures: Model, verifications and applications. Coast Eng, submitted
11 Wang J G, Karim M, Lin P. Analysis of seabed instability using element free Galerkin method. Ocean Eng, 2007, 34(2): 247–260
12 Luan M T, Qu P, Yang Q. Wave-induced dynamic response of seabed around submarine pipeline. Chin J Rock Mech Eng, 2008, 27(4): 789–795
13 Terzaghi K. Erdbaumechanik auf Bodenphysikalischer Grundlage. Vienna: F. Duticke, 1925
14 Biot M A. General theory of three dimensional consolidation. J Appl Phys, 1941, 12(2):155–164
15 Biot M A. Theory of propagation of elastic waves in an unsaturated porous solid, part I: Low frequency range. J Acoust Soc, Am, 1956, 28: 168–177
16 Sloan S W, Abbo A J. Biot consolidation analysis with automatic time stepping and error control part 1: Theory and implementation. Int J Num Anal Meth Geomech, 1999, 23(6): 467–492
17 Cavalcanti M C, Telles J C F. Biot's consolidation theory–application of bem with time independent fundamental solutions for poro-elastic saturated media. Eng Anal Bound Elem, 2003, 27(2): 145–157
18 Korsawe J, Starke G, Wang W, et al. Finite element analysis of poroelastic consolidation in porous media: Standard and mixed approaches. Computer Meth Appl Mech Eng, 2006, 195(9-12): 1096–1115
19 Wang J G, Xie H, Leung C. A local boundary integral-based meshless method for Biot's consolidation problem. Eng Anal Bound Elem, 2009, 33(1): 35–42
20 Ferronato M, Castelletto N, Gambolati G. A fully coupled 3-d mixed finite element model of Biot consolidation. J Comput Phys, 2010, 229(12): 4813–4830
21 Hua L. Stable element-free galerkin solution procedures for the coupled soilcpore fluid problem. Int J Num Meth Eng, 2011, 86(8): 1000–1026
22 Zienkiewicz O C, Chang C T, Bettess P. Drained, undrained, consolidating and dynamic behaviour assumptions in soils. Geotechnique, 1980, 30(4): 385–395
23 Ou Jianhua. Three-dimensional numerical modeling of interaction between soil and pore fluid. Doctoral Dissertation. Birmingham: University of Birmingham, 2009
24 Ye J H, Jeng D-S. Effects of bottom shear stresses on the wave-induced dynamic response in a porous seabed: PORO-WSSI (shear) model. Acta Mech Sin, 2012, 27(6): 898–910
25 Wang H F. Theory of Linear Poroelasticity with Application to Geomechanics and Hydrogeology. Princeton: Princeton University Press, 2000
26 Chung S G, Kim S K, Kang Y J, et al. Failure of a breakwate founded on a thick normally consolidated clay layer. Geotechnique, 2006, 56(3): 3 93–409
27 Zhang F G, Ge Z J. A study on some causes of rubble mound breakwater failure. China Ocean Eng, 1996, 10(4): 473–481
28 Zen K, Umehara Y, Finn W D L. A case study of the wave-induced liquefactionof sand layers under damaged breakwater. In: Proceeding 3rd Canadian Conference on Marine Geotechnical Engineering, St. John's, Newfoundland, 1985. 505–520
29 Wang J G, Zhang B, Nogami T. Wave-induced seabed response analysis by radial point interpolation meshless method. Ocean Eng, 2004, 31(1): 21–42
30 Ulker M B C, Rahman M S, Guddati M N.. Wave-induced dynamic response and instability of seabed around caisson breakwater. Ocean Eng, 2009, 37(17-18): 1522–1545
31 Tsai C P, Lee T L. Standing wave induced pore pressure in a porous seabed. Ocean Eng, 1995, 22(6): 505–517
32 Lin Z P, Liu P L-F. Internal wave-maker for navier-stokes equations models. J Waterway, Port, Coastal, Ocean Eng, 1999, 99(4): 207–215
33 Okusa S. Wave-induced stress in unsaturated submarine sediments Geotechnique, 1985, 35(4): 517–532
34 Young Y L, White J A, Xiao H et al. Liquefaction potential of coastal slopes induced by solitary waves. Acta Geotech, 2009, 4(1): 17–34
35 Xiao H, Young Y L, Prevost J H. Parametric study of breaking solitary wave induced liquefaction of coastal sandy slopes. Ocean Eng, 2010, 37(17-18): 1546–1553
36 Zhang X Y, Lee F H, Leung C F. Response of caisson breakwater subjected to repeated impulsive loading. Geotechnique, 2009, 59(1): 3–16